THE SIGNATURE OF SEA SPRAY IN THE HEXOS TURBULENT HEAT FLUX DATA

EDGAR L ANDREAS*
U.S. Army Cold Regions Research and Engineering Laboratory, 72 Lyme Road, Hanover, New Hampshire 03755-1290, U.S.A.

JANICE DECOSMO**
Geophysics Program, University of Washington, Box 351650, Seattle, Washington 98195-1650 U.S.A.

(Received in final form 3 July 2001)

Abstract. The role of sea spray in transferring heat and moisture across the air-sea interface has remained elusive. Some studies have reported that sea spray does not affect the turbulent air-sea heat fluxes for 10-m wind speeds up to at least 25 m s^{-1}, while others have reported important spray contributions for wind speeds as low as 12 m s^{-1}. One goal of the HEXOS (Humidity Exchange over the Sea) program was to quantify spray's contribution to the turbulent air-sea heat fluxes, but original analyses of the HEXOS flux data found the spray signal to be too small to be reliably identified amid the scatter in the data. We look at the HEXOS data again in the context of the TOGA-COARE bulk flux algorithm and a sophisticated microphysical spray model. This combination of quality data and state-of-the-art modelling reveals a distinct spray signature in virtually all HEXOS turbulent heat flux data collected in winds of 15 m s^{-1} and higher. Spray effects are most evident in the latent heat flux data, where spray contributes roughly 10% of the total turbulent flux in winds of 10 m s^{-1} and between 10 and 40% in winds of 15–18 m s^{-1}. The spray contribution to the total sensible heat flux is also at least 10% in winds above 15 m s^{-1}. These results lead to a new, unified parameterization for the turbulent air-sea heat fluxes that should be especially useful in high winds because it acknowledges both the interfacial and spray routes by which the sea exchanges heat and moisture with the atmosphere.

Keywords: Air-sea interaction, COARE algorithm, HEXOS, Sea spray, Turbulent heat flux.

1. Introduction

Despite 50 years of research and speculation, the question of whether sea spray plays any role in the air-sea transfer of heat and moisture still has no incontrovertible answer. For example, on combining modelling and open-ocean observations in 10-m winds no higher than 12 m s^{-1}, Ling (1993) states that spray droplets are 'a major source of atmospheric moisture and latent heat'. But Makin (1998) concluded from his modelling that 'for wind speeds below 18 m s^{-1} ... there is no drastic impact of spray on heat and moisture fluxes'. He goes on to say that his

* E-mail: eandreas@crrel.usace.army.mil
** E-mail: janice@geophys.washington.edu

Boundary-Layer Meteorology **103:** 303–333, 2002.

modelling does suggest that 'the impact of sea spray becomes significant at wind speeds of about 25 m s^{-1} and above'.

Such diverse opinions are fairly common in this field. Hasse (1992) uses three distinct arguments – an energy constraint, the total surface area of spray droplets, and the evaporation implied by the sea-salt aerosol – to make simple estimates of spray's impact and concludes that spray makes negligible contributions to surface evaporation 'except perhaps for hurricane wind strength'. Andreas (1994a), however, discusses flaws in Hasse's arguments and, while not reporting unequivocal evidence of spray's role, concludes 'we cannot so easily discount sea spray as an important agent for air-sea heat and moisture transfer'.

Andreas's (1992) spray model, which predicts that spray sensible and latent heat fluxes could be 10–15% of the magnitude of the usual interfacial, or turbulent, fluxes for wind speeds of 15–20 m s^{-1}, provoked another exchange. Katsaros and de Leeuw (1994) questioned several of Andreas's choices and assumptions and especially criticized him for ignoring the HEXOS (the Humidity Exchange over the Sea experiment) results, which, though available in preliminary form at the time, were not yet published in a refereed journal (i.e., DeCosmo et al., 1996). Indeed, the HEXOS heat flux data do not show the dramatic increase in sensible and latent heat transfer coefficients with wind speed for 10-m speeds up to 18 m s^{-1} (Katsaros and de Leeuw, 1994; DeCosmo et al., 1996; Smith et al., 1996) that scientists had been expecting since Bortkovskii's (1987) Figure 3.10 fueled this spray controversy.

In his reply to Katsaros and de Leeuw (1994), Andreas (1994b) argued that, in general, his model is compatible with the HEXOS results but offered to test that model point-by-point against the HEXOS heat flux data. This paper describes our point-by-point reanalysis of DeCosmo's (1991) HEXOS flux data in the context of Andreas's (1992) spray model.

Our goals are two. First, we want to see whether Andreas's (1992) spray model is compatible with the HEXOS data. Does it really predict spray fluxes that are much too large, as Katsaros and de Leeuw (1994) contend? To evaluate this concern, we combine the Andreas spray model with estimates of the interfacial component of the fluxes from a state-of-the-art surface flux algorithm, the COARE algorithm from Fairall et al. (1996b). We find in run-by-run simulations of the HEXOS sensible and latent heat flux data that, by including the modelled spray fluxes, we reproduce the HEXOS measurements with better accuracy than with the Fairall et al. or Zeng et al. (1998) interfacial flux algorithms alone. In other words, when viewed in the context of Andreas's model, there is a distinct spray signature in the HEXOS sensible and latent heat flux data.

This result leads to our second goal. We use the HEXOS data and Andreas's (1992) spray model to learn how to partition the total turbulent air-sea fluxes into interfacial and spray components. This analysis results in a new formulation for the air-sea fluxes of sensible and latent heat that is more appropriate than the bulk-aerodynamic method in winds, nominally, above 15 m s^{-1}.

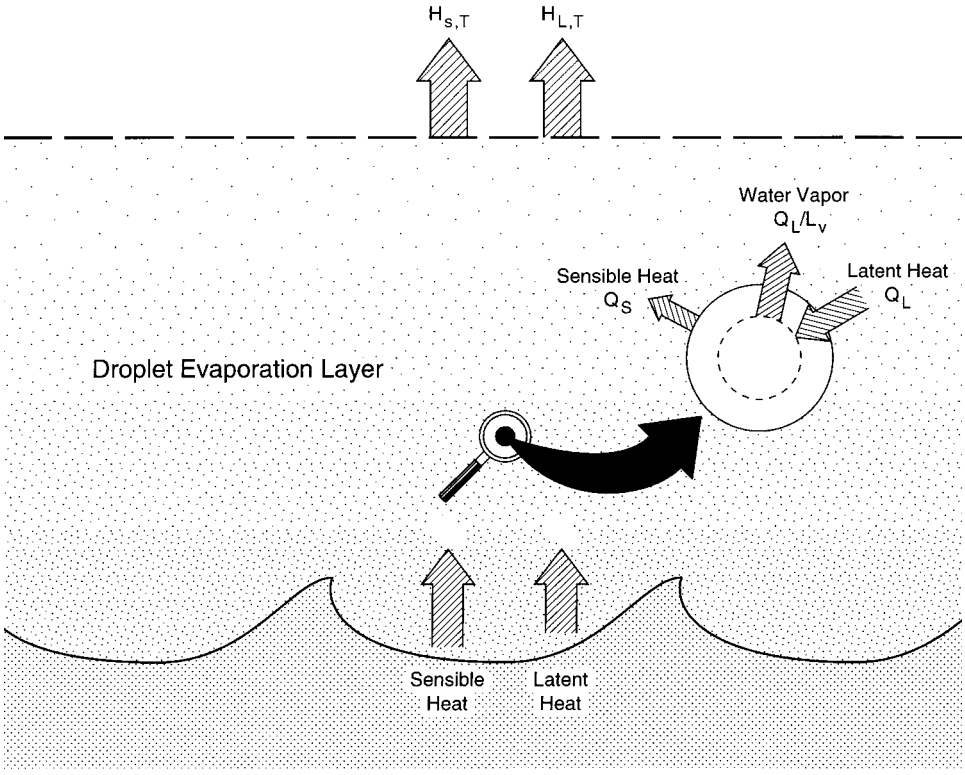

Figure 1. Our conceptual picture of processes in the droplet evaporation layer. The ocean exchanges sensible and latent heat through turbulent processes at its interface. The spray droplets also exchange water vapour and sensible and latent heat. The fluxes at the top of the DEL result from these several processes.

2. Spray Droplet Microphysics

Andreas's (1992) spray flux model uses explicit microphysical modelling to predict the thermal and size evolution of individual sea spray droplets (Andreas, 1989, 1990). Figure 1 depicts our conceptual view of the heat transfer processes in the near-surface air over the ocean and identifies the variables that the microphysical modelling can predict.

As Figure 1 shows, the ocean is always exchanging sensible (H_s) and latent (H_L) heat at its surface through turbulence. We call these the turbulent or interfacial fluxes. If the wind is strong enough to create waves, whitecaps, and the resulting sea spray, the ocean's effective surface area increases. We thus expect the transfers of sensible (Q_S) and latent (Q_L) heat at the surface of these spray droplets to augment the interfacial fluxes if the total surface area of the spray becomes a significant fraction of the area of the underlying ocean surface.

The majority of the spray transfer occurs within a droplet evaporation layer (DEL) approximately one significant wave height thick (Andreas et al., 1995).

If the ocean is warmer than the air, a spray droplet, which starts with the same temperature as the ocean surface, loses sensible heat in the DEL. If the relative humidity in the DEL is less than about 98% (because of salinity effects on vapour pressure), the droplet also begins evaporating. The microphysical modelling, as we will show, lets us predict the associated spray sensible (Q_S) and latent (Q_L) heat fluxes.

The evaporating spray extracts latent heat from the DEL but provides water vapour. Eddy-correlation instruments placed just above the DEL would thus measure total sensible ($H_{s,T}$) and latent ($H_{L,T}$) heat fluxes that reflect these combined interfacial and spray fluxes. Clearly, $H_{s,T}$ and $H_{L,T}$ provide the lower flux boundary condition for the marine boundary layer. Our objective is therefore to develop a formulation for $H_{s,T}$ and $H_{L,T}$ that recognizes spray's role in air-sea heat and moisture exchange.

When it forms, a sea spray droplet has the temperature T_w and salinity S of the ocean's surface. But once formed, it evolves toward equilibrium with its new environment. Starting with the microphysical equations in Pruppacher and Klett (1978), Andreas (1989) develops a model to track the size and thermal evolution of sea spray droplets.

In the initial stages of a droplet's thermal evolution, its temperature (T) approximately obeys (Andreas, 1989, 1990; Andreas and DeCosmo, 1999)

$$\frac{T(t) - T_{ev}}{T_w - T_{ev}} = \exp(-t/\tau_T), \tag{1}$$

where t is the time since the droplet formed and τ_T is an e-folding time. Here also, T_{ev} is a quasi-equilibrium temperature that the droplet falls to before evaporation begins in earnest (Andreas 1995, 1996; Kepert, 1996). We thus call this the evaporating temperature.

Likewise, during the initial evaporating period, the radius (r) of a spray droplet with initial radius r_0 approximately follows (e.g., Andreas, 1989)

$$\frac{r(t) - r_0}{r_0 - r_{eq}} = \exp(-t/\tau_r), \tag{2}$$

where τ_r is another e-folding time and r_{eq} is the droplet's equilibrium radius. Andreas's (1989, 1990, 1992) microphysical model computes T_{ev}, r_{eq}, τ_T, and τ_r.

Earlier analyses (e.g., Andreas, 1990, 1992) convinced us that only spray droplets with initial radii between about 1 and 500 μm can be important in transferring heat and moisture across the air-sea interface. Smaller droplets simply do not carry enough of either constituent, and larger droplets fall back into the sea before transferring much heat or moisture (e.g., Andreas, 1992; Andreas et al., 1995). Figure 2 demonstrates some of these conclusions, as do the models of Rouault et al. (1991), Edson and Fairall (1994), and Van Eijk et al. (2001). Andreas (1990, 1992) and Andreas et al. (1995) show similar plots for other conditions.

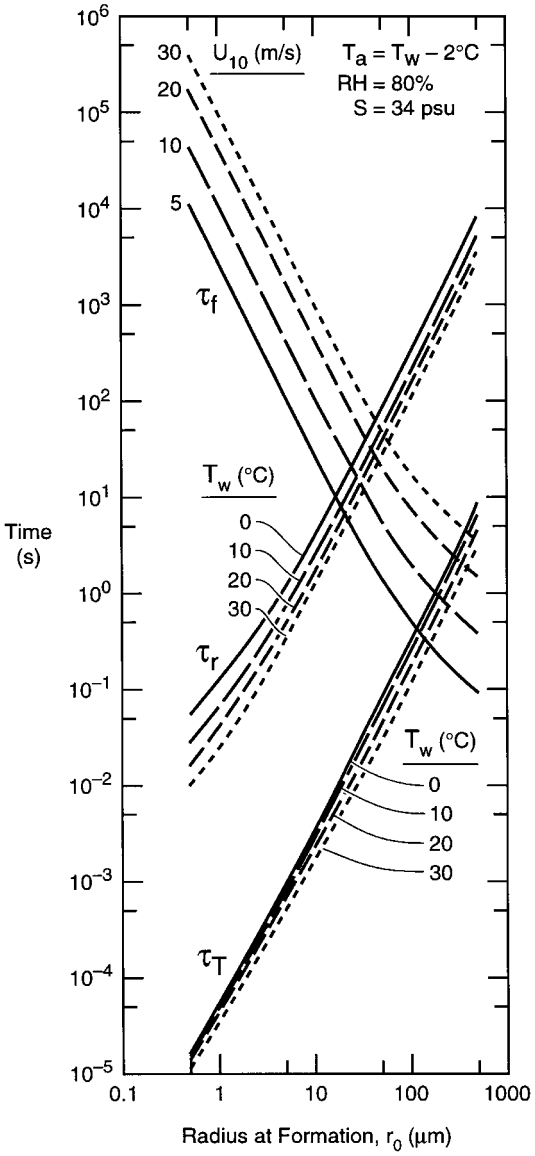

Figure 2. Spray droplet e-folding times for temperature (τ_T) and size (τ_r) evolution as a function of initial droplet radius (r_0) computed with Andreas's (1989) microphysical model. Surface water temperatures (T_w, also initial droplet temperature) are 0°, 10°, 20°, and 30 °C, as noted. For each case, the air temperature (T_a) is 2 °C less than the water temperature. τ_f is the time required for a droplet of radius r_0 to fall one significant wave amplitude (i.e., $A_{1/3}$) in still air. $A_{1/3}$ depends on the 10-m wind speed (U_{10}). The relative humidity (RH) is always 80%, the surface salinity (S) is 34 psu, and the barometric pressure is 1000 hPa.

Figure 2 shows the microphysical time scales τ_T and τ_r for a 30 °C range in seawater (or air) temperature. The first conclusion obvious in Figure 2 is that the thermal evolution and the moisture evolution of a spray droplet are decoupled: τ_r is three orders of magnitude longer than τ_T for all droplet radii. That is, droplets exchange sensible heat much more rapidly than they exchange latent heat. As a result, the relative humidity has no effect on τ_T, and the water temperature T_w has no effect on τ_r since a droplet is at T_{ev} while it evaporates.

The second conclusion we can draw from Figure 2 is that τ_T and, especially, τ_r decrease as the air temperature increases. The exponential dependence of the saturation vapour pressure on temperature explains this effect. Essentially, warmer droplets exchange vapour with their environment more rapidly than cooler ones (e.g., Bohren, 1987, p. 20) and thereby can reach equilibrium faster.

To use τ_T and τ_r to judge which spray droplets have the most potential for transferring heat and moisture in the DEL requires a dynamic time scale that parameterizes how much time the droplets have for any such exchange. Andreas (1992) introduces

$$\tau_f = A_{1/3}/u_f(r_0) \tag{3}$$

for this purpose. Here $A_{1/3}$ is the significant wave amplitude, which over the open ocean can be estimated as (e.g., Kinsman, 1965, p. 391; Wilson, 1965; Earle, 1979)

$$A_{1/3} = 0.015U_{10}^2. \tag{4}$$

This gives $A_{1/3}$ in metres for the 10-m wind speed U_{10} in m s^{-1}. Also in (3), $u_f(r_0)$ is the droplet fall speed in still air (Friedlander, 1977, p. 105; Andreas, 1989, 1990). We therefore interpret (3) as the time required for a droplet formed $A_{1/3}$ above the surface to fall back into the sea.

Lagrangian and Eulerian models of spray droplet dispersion by Edson (Andreas et al., 1995; Edson et al., 1996) and Van Eijk et al. (2001), respectively, corroborate that $A_{1/3}$ is a relevant height scale in the DEL. Mestayer et al. (1996), however, suggest that $A_{1/3}$ is too large for this scale; while Kepert et al. (1999) suggest that it is too small.

Figure 2 also plots τ_f as a function of r_0 with U_{10} as a parameter. Droplets with small radii have τ_f values of many hundreds of seconds. In our application, these are suspended in the air indefinitely and can transfer their entire loads of sensible heat and moisture to the atmosphere. For droplet radii between 10 and 100 μm, however, τ_f and τ_r cross. We infer that droplets for which $\tau_f > \tau_r$ transfer most of their moisture to the atmosphere before falling back into the sea, while droplets for which $\tau_f < \tau_r$ fall back into the sea before transferring much moisture. Similarly, the τ_f lines cross the τ_T lines between 100 and 500 μm. Droplets to the left of this crossing transfer most of their sensible heat to the air before returning to the sea, while droplets to the right fail to transfer much sensible heat. These considerations form the basis of the Andreas (1992) spray flux model.

3. Spray Heat Flux Model

A spray droplet starts with the same temperature as the seawater surface, T_w. After a flight in the DEL of approximate duration τ_f, from (1), it falls back into the sea with temperature

$$T(\tau_f) = T_{ev} + (T_w - T_{ev}) \exp(-\tau_f/\tau_T). \tag{5}$$

The temperature difference $T_w - T(\tau_f)$ drives the rate at which all droplets of initial radius r_0 transfer sensible heat to the air. Consequently, from (5), this rate is

$$Q_S(r_0) = \rho_s c_{ps}(T_w - T_{ev})[1 - \exp(-\tau_f/\tau_T)] \left(\frac{4\pi r_0^3}{3}\frac{\mathrm{d}F}{\mathrm{d}r_0}\right). \tag{6}$$

Here, ρ_s is the density of seawater, c_{ps} is the specific heat of seawater at constant pressure, and $\mathrm{d}F/\mathrm{d}r_0$ is the rate at which droplets of radius r_0 are produced at the sea surface. In (6), Q_S has units of a heat flux per increment in droplet radius, W m^{-2} μm^{-1}.

Similar arguments lead to an estimate of the spray latent heat flux. For $\tau_f \leq \tau_r$, (2) implies that, after a flight of duration τ_f, a droplet with initial radius r_0 falls back into the sea with radius

$$r(\tau_f) = r_{eq} + (r_0 - r_{eq}) \exp(-\tau_f/\tau_r). \tag{7}$$

These droplets, therefore, transfer latent heat at a rate

$$Q_L(r_0) = \rho_s L_v \left\{1 - \left[\frac{r(\tau_f)}{r_0}\right]^3\right\} \left(\frac{4\pi r_0^3}{3}\frac{\mathrm{d}F}{\mathrm{d}r_0}\right) \qquad \text{for } \tau_f \leq \tau_r, \tag{8a}$$

where L_v is the latent heat of vaporization.

If the relative humidity is 95% or less, droplets for which $\tau_f > \tau_r$ will have experienced at least two-thirds of their potential moisture loss before they fall back into the sea (Andreas, 1992). As Figure 2 suggests, most will have lost even more water. For these droplets, we simply assume that $\tau_f \gg \tau_r$ and, from (7), approximate their rate of latent heat exchange as

$$Q_L(r_0) = \rho_s L_v \left[1 - \left(\frac{r_{eq}}{r_0}\right)^3\right] \left(\frac{4\pi r_0^3}{3}\frac{\mathrm{d}F}{\mathrm{d}r_0}\right) \qquad \text{for } \tau_f > \tau_r. \tag{8b}$$

Our candidate for the spray generation function $\mathrm{d}F/\mathrm{d}r_0$ in (6) and (8) is the function Andreas (1992) used originally. This function is based on Miller's (1987) analysis and is appropriate for 10-m winds up to 20 m s^{-1}. We will refer to this as the Andreas (1992) spray generation function. Van Eijk et al. (2001) likewise conclude that this function is a good choice for spray modelling.

By integrating $Q_S(r_0)$ and $Q_L(r_0)$ over all r_0, we get what we call 'nominal' values for the spray sensible and latent heat fluxes:

$$\bar{Q}_S = \int_{r_1}^{r_2} Q_S(r_0)\mathrm{d}r_0, \tag{9a}$$

$$\bar{Q}_L = \int_{r_1}^{r_2} Q_L(r_0)\mathrm{d}r_0, \tag{9b}$$

where r_1 and r_2 are the smallest and largest droplet radii that contribute to the integrals. For the Andreas (1992) function, r_1 and r_2 are, respectively, 1.6 and 500 μm. Both $\bar{Q}_S$ and $\bar{Q}_L$ have dimensions of a heat flux, W m^{-2}. Because the microphysical model is theoretically based, $\bar{Q}_S$ and $\bar{Q}_L$ have proper dependencies on temperature, humidity, and wind speed. They are still 'nominal' fluxes, though, because of the approximations in (6) and (8) and, especially, because of the persistent uncertainty in the spray generation function $\mathrm{d}F/\mathrm{d}r_0$ (e.g., Katsaros and de Leeuw, 1994; Andreas et al., 1995; Mestayer et al., 1996; Andreas, 1998).

Andreas (1992, 1994b), Andreas and DeCosmo (1999), and Andreas et al. (1995) tabulate and plot calculations of $\bar{Q}_S$ and $\bar{Q}_L$ for various conditions. Andreas (1992) implicitly assumes that $\bar{Q}_S$ and $\bar{Q}_L$ add directly to H_s and H_L, respectively, to produce $H_{s,T}$ and $H_{L,T}$ (in Figure 1). Fairall et al. (1994), however, point out that, since the DEL must supply the latent heat to produce $\bar{Q}_L$, $H_{s,T}$ must decrease by this amount. In addition, Katsaros and DeCosmo (1990), Katsaros and de Leeuw (1994), and DeCosmo et al. (1996) describe an additional coupling between the temperature and moisture fields when spray is present. Because evaporating spray cools the DEL, the difference between the sea and the near-surface air temperatures should increase. This coupling creates a feedback that would augment H_s. Mestayer and Lefauconnier (1988) document that, in a wind-water tunnel, the near-surface air is cooler when spray is present than when it is not. Rouault et al. (1991) and Edson et al. (1996) likewise demonstrate this positive feedback between spray and interfacial processes with Eulerian and Lagrangian spray models, respectively.

Thus, building on the ideas by Fairall et al. (1994) and the recognition that the spray couples the temperature and moisture fields, Andreas and DeCosmo (1997, 1999) and Edson and Andreas (1997) hypothesize that the total turbulent fluxes at the top of the DEL (see Figure 1) can be partitioned as

$$H_{L,T} = H_L + \alpha\bar{Q}_L, \tag{10a}$$

$$H_{s,T} = H_s + \beta\bar{Q}_S - (\alpha - \gamma)\bar{Q}_L, \tag{10b}$$

where $\bar{Q}_L$ and $\bar{Q}_S$ come from (9) and H_s and H_L come from bulk aerodynamic estimates. Here also, α, β, and γ are presumed to be small, non-negative constants that tune the nominal spray fluxes $\bar{Q}_L$ and $\bar{Q}_S$ to data. (Note that the α terms in

(10) have a sign convention that is opposite to the one used by Edson and Andreas (1997) and Andreas and DeCosmo (1999).)

In (10a), the α term simply models the latent heat flux coming out the top of the DEL that the spray has contributed. This quantity of latent heat $\alpha \bar{Q}_L$ must appear with the opposite sign in the $H_{s,T}$ Equation, (10b), to reflect the sensible heat that the evaporating spray extracts from the temperature field.

Because the evaporating spray cools the DEL and thereby increases the near-surface sea-air temperature difference, we add back in (10b) some of the latent heat responsible for this cooling as $\gamma \bar{Q}_L$. That is, we expect $\gamma \leq \alpha$. In essence, this term reflects the fact that, because of the spray, temperature and humidity profiles in the DEL do not follow the usual Monin–Obukhov similarity forms when predicted from meteorological variables measured above the DEL (cf. Smith, 1990; Andreas et al., 1995). Consequently, the bulk aerodynamic formulae that we will discuss shortly require some nudging to predict H_s and H_L correctly in the presence of spray. This is the purpose of the $\gamma \bar{Q}_L$ term.

Similarly, the spray latent heat flux moistens the DEL and, therefore, should decrease the humidity gradient that drives H_L. But we need not explicitly account for this feedback in (10a), as we do with the $\gamma \bar{Q}_L$ term in (10b), because α implicitly includes it.

The final spray term in the $H_{s,T}$ equation is $\beta \bar{Q}_S$. This simply shows that, if spray starts with a temperature different from the air (actually, different from T_{ev}), it also transports sensible heat across the air-sea interface. In his spray model, Makin (1998), for example, ignores this contribution, while Andreas and Emanuel (1999) highlight it as the likely route through which spray contributes to the total sea-air enthalpy flux.

Although our (10) derives from the ideas contained in Fairall et al. (1994), we interpret α and β differently and add the γ term that they do not have. The model by Fairall et al. and related models by Kepert et al. (1999) and Bao et al. (2000) include full boundary-layer schemes that couple the air-sea exchange to the evolution of boundary-layer variables in the presence of spray. These coupled models inherently track the feedbacks between spray and the interfacial fluxes that we find necessary to parameterize with α and γ in our more simple model.

We do, nevertheless, have a fundamental philosophical difference with Fairall et al. (1994), Kepert et al. (1999), and Bao et al. (2000). On the basis of feedback arguments, all three groups have α and β bounded between 0 and 1. To us, this assumption implies that these authors feel that they know $\bar{Q}_S$ and $\bar{Q}_L$ quite well. In particular, they are assuming implicitly that the real spray sensible and latent heat contributions are no larger than $\bar{Q}_S$ and $\bar{Q}_L$, respectively. In light of the large uncertainties that still remain in the magnitude of the spray generation function, we do not feel justified in assuming that we know $\bar{Q}_S$ and $\bar{Q}_L$ this well. Rather, our philosophy is simply to let α, β, and γ be non-negative and allow the data to tell us how big these constants need to be. We base our estimates of α, β, and

γ on DeCosmo's (1991) HEXOS data and the Andreas (1992) spray generation function.

Those familiar with the HEXOS results may think this is a pointless endeavour. After all, DeCosmo et al. (1996), Smith et al. (1996), and Makin (1998) all conclude that there is no spray effect evident in the HEXOS eddy-correlation measurements of heat flux through the entire range of available wind speeds, up to 18 m s^{-1}. This conclusion basically rests on the observation that the 10-m, neutral-stability transfer coefficients for sensible (C_{HN10}) and latent (C_{EN10}) heat computed from the HEXOS measurements seem to be constant with wind speed. But Liu et al. (1979) actually predict that C_{HN10} and C_{EN10} should decrease with increasing wind speed for 10-m winds above 5 m s^{-1} if the transfer is through interfacial processes alone. DeCosmo et al. do qualify their conclusion that the HEXOS heat fluxes show no spray effects for wind speeds up to 18 m s^{-1} by pointing out that their 15% experimental error did not rule out spray effects of this magnitude. In fact, their data suggest, roughly, a 10% increase in the latent heat transfer coefficient for their highest wind speeds. Given the experimental error, however, DeCosmo et al. preferred to leave that question open until more data or a theoretical model could provide a way to extract the spray signal from the measurements. We believe we now have such a model.

The best way to test for a spray signal in the HEXOS data is to see whether current bulk aerodynamic models reproduce the measured scalar fluxes. The bulk aerodynamic formulation for the turbulent heat fluxes is

$$H_s = \rho_a c_p C_{H10} U_{10} (T_w - T_{10}), \tag{11a}$$

$$H_L = \rho_a L_v C_{E10} U_{10} (q_w - q_{10}). \tag{11b}$$

Here ρ_a is the density of moist air; c_p, the specific heat of air at constant pressure; T_{10} and q_{10}, the average air temperature and specific humidity at 10 m; and q_w, the specific humidity of air at the sea surface.

The bulk transfer coefficients for sensible and latent heat appropriate for a reference height of 10 m derive from the roughness lengths for wind speed (z_0), temperature (z_T), and humidity (z_q) according to

$$C_{H10} = \frac{k^2}{[\ln(10/z_0) - \psi_m(10/L)][\ln(10/z_T) - \psi_h(10/L)]}, \tag{12a}$$

$$C_{E10} = \frac{k^2}{[\ln(10/z_0) - \psi_m(10/L)][\ln(10/z_q) - \psi_h(10/L)]}. \tag{12b}$$

Here, k (= 0.4) is the von Kármán constant, and L, the Obukhov length, is a stability parameter (defined in the appendix). Also in (12), ψ_m and ψ_h are empirical stability corrections. For these, we use the functions that DeCosmo (1991) used in her original analysis. In unstable conditions (i.e., $L < 0$)

$$\psi_m(10/L) = 2\ln[(1 + x)/2] + \ln[(1 + x^2)/2] - \arctan(x) + \pi/2, \tag{13a}$$

$$\psi_h(10/L) = 2\ln[(1 + x^2)/2], \tag{13b}$$

where

$$x = [1 - 16(10/L)]^{1/4}. \tag{13c}$$

In stable conditions (i.e., $L > 0$),

$$\psi_m(10/L) = \psi_h(10/L) = -5(10/L). \tag{14}$$

These are all fairly standard equations. The key, therefore, to the bulk parameterization is deciding how to set z_0, z_T, and z_q. For our first estimate of z_T and z_q, we use the COARE version (Fairall et al., 1996b) of the model that Liu et al. (1979; henceforth, LKB) developed. The COARE algorithm is arguably the best current model for the wind speed dependence of z_T and z_q over the ocean (e.g., Grant and Hignett, 1998; Chang and Grossman, 1999). Fairall et al. verify this algorithm, though, for winds only up to 10 m s^{-1}. The FORTRAN code for the algorithm, however, includes fitting coefficients for roughness Reynolds numbers (R_*) up to 1000, which correspond to wind speeds over the ocean at 10-m height of well over 30 m s^{-1}. (Note, $R_* = u_* z_0/\nu$, where ν is the kinematic viscosity of air.) LKB, whose model for z_T and z_q is the basis of the COARE algorithm, also imply that their model should be accurate for wind speeds up to at least 18 m s^{-1}, the upper limit of the HEXOS data and, in fact, tune it with laboratory data featuring R_* values of several hundred.

Still C. W. Fairall (pers. comm., 2000) worries that the COARE algorithm's predicted values of z_T and z_q may fall too fast for large R_* values. For the HEXOS data we use here, however, only 9 of 136 sensible heat flux values and only 12 of 233 latent heat flux values were collected in conditions with R_* larger than 100. And 189 was the maximum R_* value for the data we consider. Consequently, we seem to be using the COARE/LKB parameterization for z_T and z_q well within the range for which it was tuned.

The COARE algorithm includes parameterizations that predict the actual ocean surface temperature, which is the relevant quantity in specifying T_w and q_w in (11). This may differ from the bulk near-surface water temperature because of cool-skin and warm-layer effects (Fairall et al., 1996a). We do not, however, include these provisional parameterizations in implementing the COARE algorithm, believing that the effects they model will be small in the high winds that characterize the HEXOS data (e.g., Donlon and Robinson, 1997).

As an alternative to the COARE/LKB model for z_T and z_q, we also consider the parameterization by Zeng et al. (1998),

$$z_T = z_q = z_0 \exp[-(2.67R_*^{1/4} - 2.57)], \tag{15}$$

which is also well tested for wind speeds up to 10 m s^{-1}. The Zeng et al. parameterization is a generalization of the model that Brutsaert (1975; see also Brutsaert,

1982, p. 122 f.) originally developed from theoretical arguments and laboratory data collected over solid surfaces. Garratt (1992, p. 102) applies the Brutsaert parameterization to flow over the sea. Zeng et al. generalize Garratt's summary by setting z_T and z_q equal (in Brusaert's original formulation, they differed because of the different molecular diffusivities of heat and water vapour) and by using (15) even for aerodynamically smooth flow, where Brutsaert gives another parameterization for z_T and z_q.

Although (15) has the same form as Garratt's (1992, p. 102) models for z_T and z_q, Zeng et al. (1998) adjusted the numerical coefficients to make their parameterization produce values of C_{E10} at neutral stability (i.e., C_{EN10}) that agree with the HEXOS results of DeCosmo et al. (1996) for wind speeds above 10 m s^{-1}. That is, if the HEXOS data are influenced by spray at high winds, the Zeng et al. parameterization may be implicitly accounting for these effects. But Zeng et al. have not really tested their parameterization against the HEXOS data, only against the published HEXOS value of C_{EN10} (see their Figure 8). As with the COARE algorithm, Zeng et al. actually tested their parameterization with COARE data that include 10-m wind speeds only up to about 10 m s^{-1}. Consequently, the Zeng et al. parameterization is comparable to the COARE algorithm: both are theoretically based and validated for wind speeds up to about 10 m s^{-1}, where spray has minimal effect. In essence, we are thus using the COARE and Zeng et al. algorithms to look for spray effects in the HEXOS data but may also be highlighting differences between two state-of-the-art bulk flux algorithms.

Both the COARE (Fairall et al., 1996b) and Zeng et al. (1998) algorithms include a parameterization for z_0 that is appropriate over the open ocean. The HEXOS data, however, were collected on Meetpost Noordwijk in the North Sea off the Dutch coast, where the water is only 18 m deep. Because the COARE and Zeng et al. z_0 algorithms are inappropriate in such shallow water, to estimate z_0 we use the actual HEXOS analysis of the 10-m, neutral-stability drag coefficient (Smith et al., 1992),

$$C_{DN10} \equiv \left(\frac{u_*}{U_{N10}}\right)^2 = (0.27 + 0.116U_{N10}) \times 10^{-3}, \tag{16}$$

where U_{N10} is the neutral-stability wind speed at 10 m in m s^{-1}. The roughness length z_0 in metres then comes from

$$z_0 = 10\exp(-kC_{DN10}^{-1/2}). \tag{17}$$

DeCosmo (1991) and Maat et al. (1991) also parameterize the HEXOS values of C_{DN10} and z_0 in terms of sea-state parameters such as significant wave height ($H_{1/3}$), the phase speed of the dominant waves (C_p), and u_*. Because their data were more limited in number than the set that Smith et al. (1992) used, and because C_p is not generally available for all the HEXOS runs that we consider, we prefer the Smith et al. relation, (16).

Geernaert et al. (1986) report that their measurements at another site in the North Sea show a dependence on wind speed similar to that in (16). This wind dependence is stronger than ones in analogous relations derived over the open ocean – for example, compare Large and Pond (1981), who found

$$C_{DN10} = 1.20 \times 10^{-3} \qquad \text{for } 4 \leq U_{N10} \leq 11 \text{ m s}^{-1}, \tag{18a}$$

$$C_{DN10} = (0.49 + 0.065U_{N10}) \times 10^{-3} \qquad \text{for } 11 \text{ m s}^{-1} \leq U_{N10}. \tag{18b}$$

The shallow HEXOS site also forces us to modify the way Andreas's (1992) original model estimates τ_f, since (4) does not provide an accurate estimate of the significant wave amplitude here. Fortunately, HEXOS scientists measured the significant wave height $H_{1/3}$ (= $2A_{1/3}$) concurrently with DeCosmo's (1991) flux measurements. Figure 3 shows the HEXOS measurements of $H_{1/3}$ and how these data compare to the prediction based on (4). Clearly, the wave growth is much less vigorous in the North Sea than it is at the same wind speed over the open ocean. Since the effects of spray on air-sea heat and moisture transfer increase with the time the spray spends in the air, and since this time is directly proportional to $A_{1/3}$ [or $H_{1/3}$; see (3)], Figure 3 implies that the HEXOS site may not exhibit spray effects as large as an open ocean site would at the same wind speed.

Figure 3 and the increased wind dependence in (16) imply that waves in the North Sea are smaller but steeper and, thus, less developed than those over the open ocean. These facts raise questions about the validity of using the Andreas (1992) spray generation function for modelling spray production in the HEXOS data set. The increased wind dependence in the drag coefficient implies steeper, slower-moving waves and increased form drag in the shallow North Sea (Geernaert et al., 1986, 1987; Smith et al., 1992). All these wave features suggest enhanced spray production though not necessarily much change in the shape of the spray size spectrum. Figure 1 in Andreas (1998), however, shows that, for all droplet radii, the spray volume flux that the Andreas (1992) spray generation function predicts is typically three times larger than the flux predicted by another realistic spray generation function that Andreas (1998) derives from observations by M. H. Smith et al. (1993). We are confident that any enhanced spray production in the North Sea will be smaller than this factor-of-three uncertainty in the spray generation function and thus negligible for our purposes.

Using (16), (17), and predictions of z_T and z_q from the COARE/LKB and Zeng et al. (1998) algorithm, we can substitute in (12) (with $10/L = 0$) to calculate theoretical values of the neutral-stability, 10-m values of the sensible and latent heat transfer coefficients, C_{HN10} and C_{EN10}, for the HEXOS site. Figure 4 shows these predictions and C_{DN10} calculated from (16). Near $U_{N10} = 7$ m s^{-1}, the COARE/LKB estimates of C_{HN10} and C_{EN10} reach maxima of 1.11×10^{-3} and 1.14×10^{-3}, respectively, very nearly the values that DeCosmo et al. (1996) report as the averages for C_{HN10} and C_{EN10} over the entire HEXOS wind speed range (i.e., 1.14×10^{-3} and 1.12×10^{-3}, respectively).

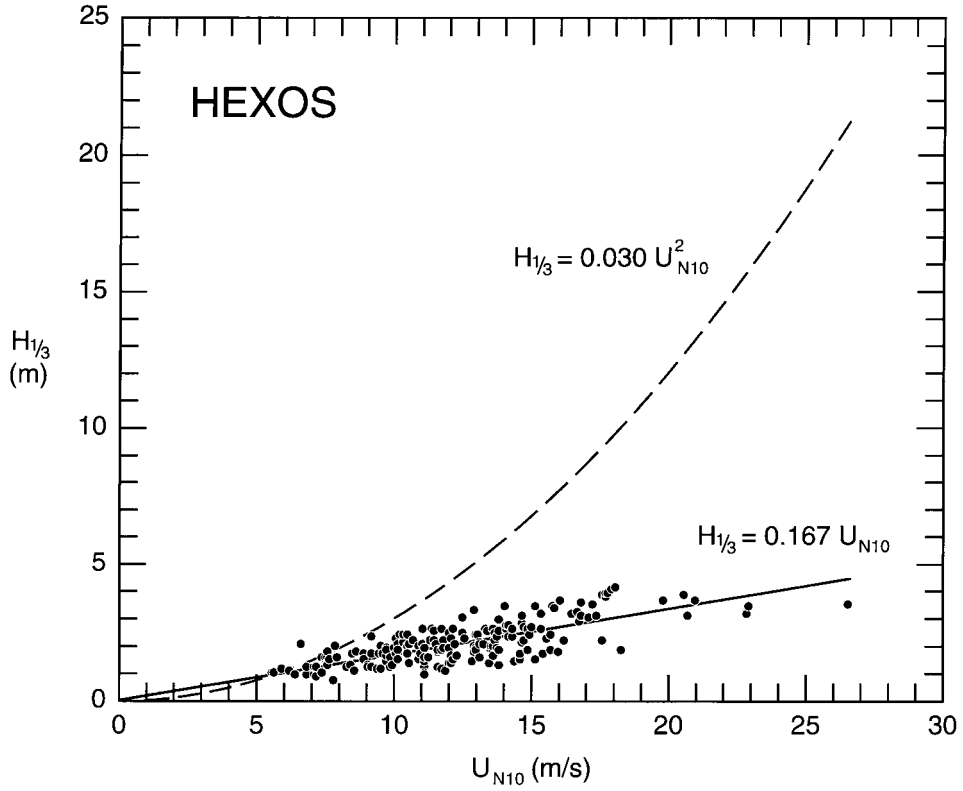

Figure 3. HEXOS measurements of significant wave height as a function of the 10-m wind speed at neutral stability. The dashed line shows the open-ocean prediction for wave height based on (4). The solid line is our best fit to the HEXOS data.

Figure 4 shows, however, that the LKB theory predicts that both C_{HN10} and C_{EN10} should decrease as U_{N10} increases beyond this maximum. If their theory is correct, we see the fallacy of concluding that there is no sea spray effect evident in the HEXOS data because the transfer coefficients do not increase dramatically with wind speed. Since the coefficients should theoretically decrease in the absence of spray effects, the reports by DeCosmo et al. (1996) and Smith et al. (1996) that both coefficients remain roughly constant up to wind speeds of 18 m s^{-1} could be evidence of enhanced heat exchange mediated by the spray.

The Zeng et al. (1998) formulation for z_T and z_q implies that, at the HEXOS site, C_{HN10} and C_{EN10} continually increase for wind speeds up to about 15 m s^{-1}, reach a maximum here of 1.30×10^{-3}, and only then begin decreasing with increasing wind speed. Ironically, though Zeng et al. explicitly adapted (15) to match the HEXOS C_{EN10} value, the value of this maximum, 1.30×10^{-3}, is about 15% larger than the averages for C_{HN10} and C_{EN10} implied by the original HEXOS analysis (DeCosmo et al., 1996). This overestimate results because properly implementing C_{EN10} and C_{HN10} parameterizations for the HEXOS site requires using z_0

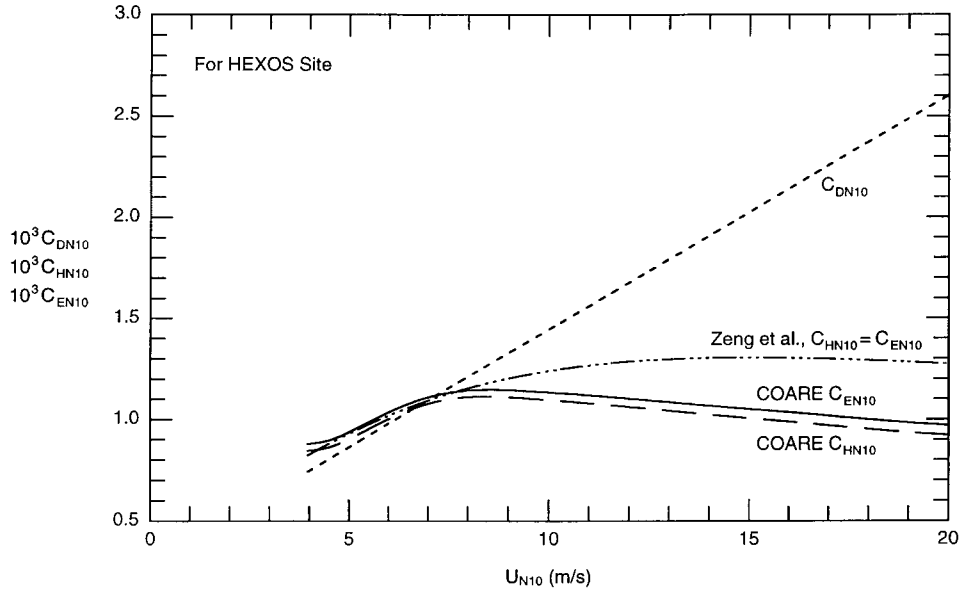

Figure 4. Theoretical predictions of C_{HN10} and C_{EN10} at the HEXOS site based on the COARE (Fairall et al., 1996b) and Zeng et al. (1998) bulk flux algorithms but with the HEXOS result (16) used to predict C_{DN10} (also shown) and z_0. U_{N10} is the wind speed that would be measured at 10 m if the atmospheric stratification were neutral.

from (16) and (17) in (12). Zeng et al., however, evidently used their open-ocean parameterization for z_0 and adjusted only z_q (and z_T) to produce a match with the HEXOS C_{EN10} value. We thus suspect that the Zeng et al. algorithm for z_T and z_q overestimates these values. We will elaborate on this observation shortly.

4. Tests with the HEXOS Data

The HEXOS heat flux data were collected expressly to study the question of spray's role in air-sea heat and moisture transfer (Katsaros et al., 1987; Mestayer et al., 1989; Smith et al., 1990, 1996). Therefore, the investigators gave careful attention to the details of measuring the turbulent fluxes by eddy-correlation in a marine environment in high winds. For example, sea salt can confound turbulent temperature measurements made with in situ sensors by collecting on the thermometer and thereby making it respond to fluctuations in both humidity and temperature (e.g., Schmitt et al., 1978; Davidson et al., 1978; Fairall et al., 1979). The HEXOS team, however, devised methods to mitigate this and other sampling problems; DeCosmo (1991), Katsaros et al. (1994), DeCosmo et al. (1996), and Smith et al. (1996) describe these innovations.

On Meetpost Noordwijk, the HEXOS flux sensors were typically between 6 and 10 m above mean sea level. If the thickness of the DEL is about one significant

wave height, as Andreas et al. (1995) suggest, Figure 3 confirms that these sensors were always above the DEL and were, thus, measuring the total turbulent fluxes, $H_{L,T}$ and $H_{s,T}$ (see (10)).

DeCosmo (1991) tabulates the turbulent flux data and the standard meteorological observations that we use in our model comparison. We have, however, manipulated these data to create physical variables that our model can use. The appendix describes this preprocessing; the result is what we mean when we henceforth refer to the 'HEXOS data'.

Figures 5 and 6 compare the measured HEXOS sensible and latent heat fluxes with the same fluxes estimated using the bulk-aerodynamic algorithms we described in the last section. Rather than plotting fluxes directly, however, we plot ratios of measured and modelled fluxes versus U_{N10}, which DeCosmo (1991) tabulates for each HEXOS run. This format readily shows whether the bulk-aerodynamic algorithm accurately describes the HEXOS measurements. If it does, the ratios of measured-to-modelled sensible (R_s) and latent (R_L) heat fluxes would tend to be about 1, and neither ratio would depend on wind speed. In other words, average values of R_s and R_L should be near 1, and the correlation coefficients for R_s versus U_{N10} and for R_L versus U_{N10} should be near 0. The model, therefore, would be correctly predicting the magnitude and explaining all the wind speed dependence in the flux measurements.

In both panels in Figure 5, however, the ratios average greater than 1; and both plots have positive slopes. In the latent heat panel, the measured fluxes are, on average, 13.3% larger than the modelled fluxes; in the sensible heat panel, they average 7.3% larger than the modelled fluxes. In the latent heat panel, all 23 cases with $U_{N10} > 15$ m s^{-1} result in measured fluxes larger than modelled fluxes. Similarly, in the sensible heat flux panel, 14 cases for which $U_{N10} > 15$ m s^{-1} show measured fluxes larger than modelled fluxes, while only four cases show the opposite.

Using the technique that Bendat and Piersol (1971, p. 126 ff.) describe for assigning a confidence interval to the correlation coefficient, we can test the hypothesis that the ratios R_s and R_L in Figure 5 are not correlated with wind speed and, thus, the hypothesis that the COARE algorithm accurately represents the HEXOS data. For the sensible heat flux plot in Figure 5, however, we reject at the 2.2% significance level the hypothesis that R_s is independent of wind speed. Similarly, for the latent heat flux plot, we reject at the 0.2% (!) significance level the hypothesis that R_L is independent of wind speed.

In summary, the COARE bulk flux algorithm (adapted for conditions in the North Sea) cannot adequately explain the magnitudes of the measured HEXOS fluxes nor their dependence on wind speed. The disparity in the latent heat flux panel in Figure 5, especially, is in the right direction to be evidence of spray effects.

As a counterpoint, we show in Figure 6 an alternative evaluation of R_s and R_L based on the Zeng et al. (1998) algorithm. Here we see the opposite trends in R_s and R_L with wind speed, though. In the latent heat flux panel, for wind speeds above 15 m s^{-1}, 16 of the 23 R_L values are less than 1. In the sensible heat flux

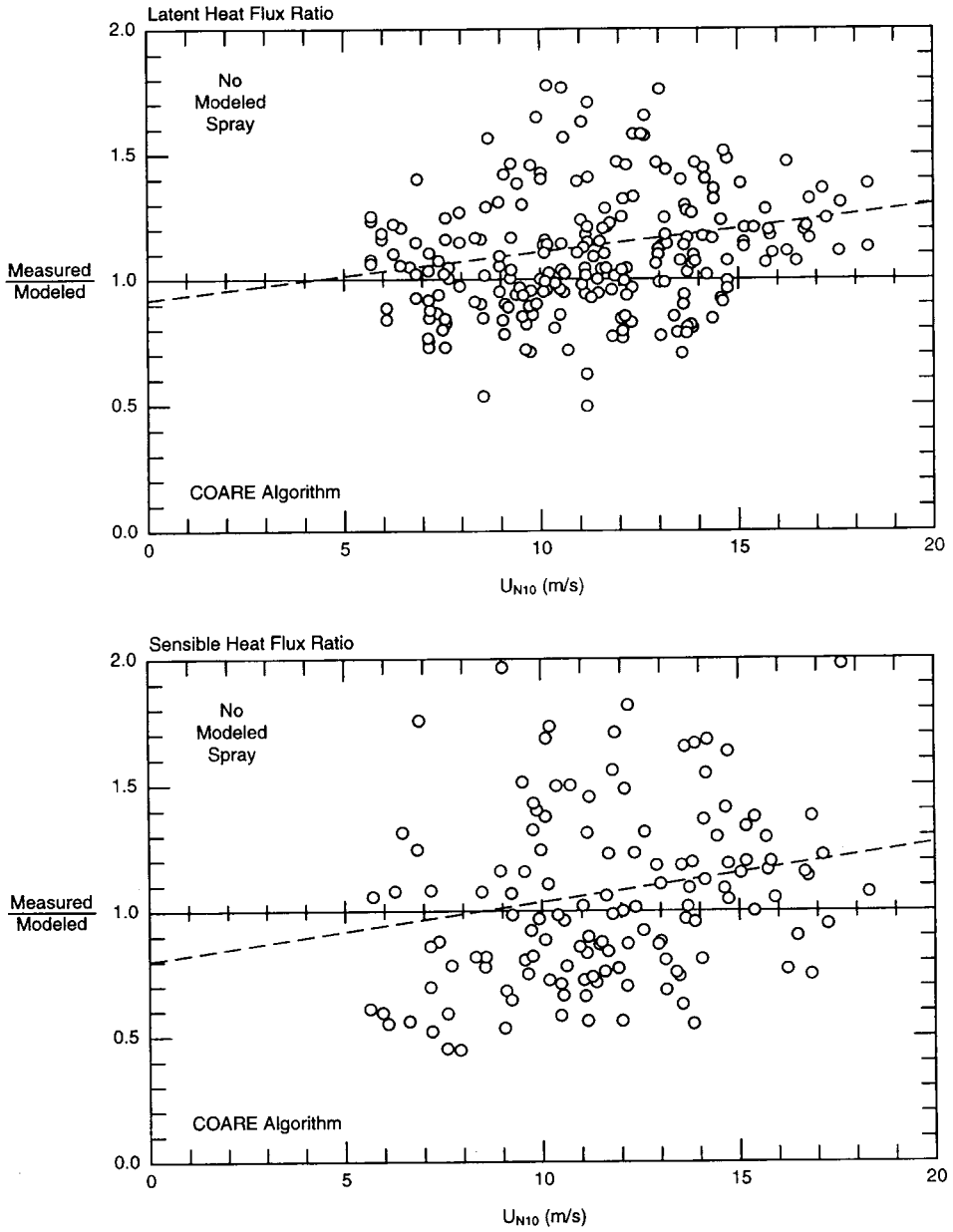

Figure 5. Ratios of HEXOS measurements of the latent and sensible heat fluxes (DeCosmo, 1991) and the corresponding fluxes modelled, basically, with the COARE algorithm (Fairall et al., 1996b). U_{N10} is the neutral-stability wind speed at 10 m. Here, the modelled fluxes have no spray contribution; $\alpha = \beta = \gamma = 0$ in (10). The dashed lines in each panel represent the best fit to the data. In the latent heat flux plot, the ratio average is 1.133, and the correlation coefficient is 0.184; in the sensible heat flux plot, the average is 1.073, and the correlation coefficient is 0.174. Note that we are looking for near-zero correlation coefficients here because these would mean that the model has explained all the wind speed dependence in the measurements.

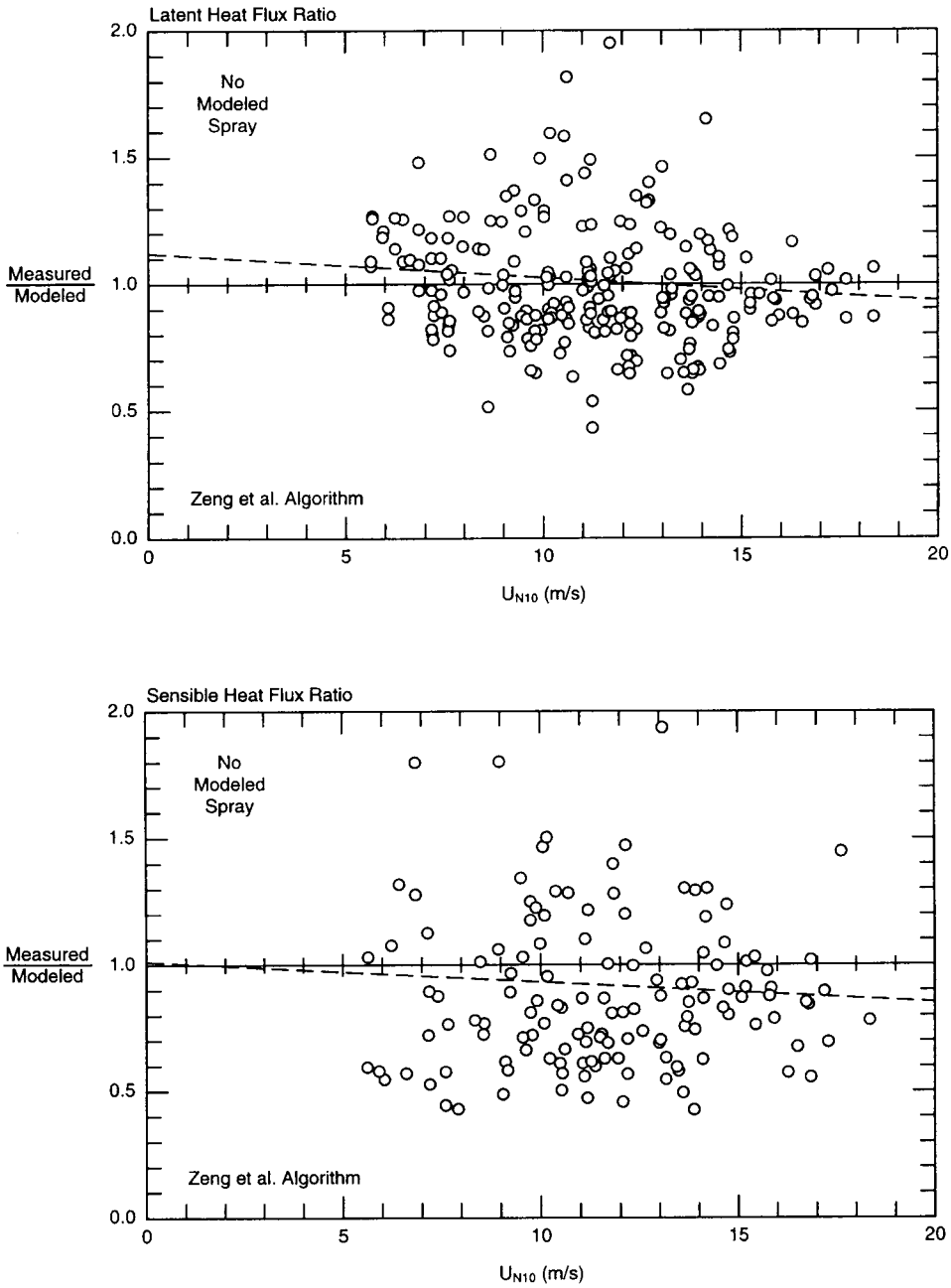

Figure 6. As in Figure 5, except here we use the Zeng et al. (1998) parameterization for z_T and z_q. In the latent heat flux plot, the ratio average is 1.010, and the correlation coefficient is -0.100; in the sensible heat flux plot, the average is 0.917, and the correlation coefficient is -0.061.

panel, again for wind speeds above 15 m s^{-1}, 15 of the 19 R_s values are less than 1.

These negative trends in R_s and R_L with wind speed in Figure 6 are statistically reliable. Again, using Bendat and Piersol's (1971, p. 126 ff.) method for evaluating the confidence interval on a correlation coefficient, we reject the hypothesis that R_s and U_{N10} in Figure 6 are uncorrelated at the 24% significance level. In other words, in light of the statistics implied by the sensible heat flux plot, there is only about a one-in-four chance that variables that are really uncorrelated could have produced this plot. From the latent heat flux plot, we similarly reject the hypothesis that R_L and U_{N10} are uncorrelated at the 6.4% significance level. That is, there is only one chance in 16 that uncorrelated variables could have produced this plot.

Presumably, because Zeng et al. (1998) tuned their algorithm to agree with the original HEXOS C_{EN10} value, it produces, on average, slightly better estimates of the HEXOS heat fluxes than does the COARE algorithm. Still, these negative trends in R_s and R_L are troubling. For the latent heat flux, especially, the trend in R_L is contrary to our conceptual picture of how spray affects latent heat transfer. If, at higher wind speeds, evaporation from spray augments the interfacial flux of latent heat measured above the DEL (see Figure 1 and Equaion (10a)), the Zeng et al. algorithm should predict the latent heat flux here correctly, since it was supposedly tuned to the HEXOS C_{EN10}, or should underpredict that flux, as the COARE algorithm does. Since the Zeng et al. algorithm overpredicts both latent and sensible heat fluxes, their algorithm evidently predicts z_T and z_q values that are too large. We, therefore, cannot reliably extrapolate the Zeng et al. algorithm beyond its validated wind speed range of about 10 m s^{-1}.

Because neither bulk flux algorithm does well in representing the HEXOS data in high winds, we augment the COARE bulk flux estimates with Andreas's (1992) spray model for $\bar{Q}_S$ and $\bar{Q}_L$ with nonzero α, β, and γ values in (10) to explicitly treat spray contributions to the HEXOS fluxes. The one difference from Andreas (1992) here is that we use actual measurements of $H_{1/3}$ (= $2A_{1/3}$), rather than (4), to estimate τ_f in (3).

Figure 7 shows how we evaluated α in (10a). As in Figure 5, the COARE bulk flux algorithm gives H_L in (10a), our spray model gives $\bar{Q}_L$, and we vary α to try to reproduce the HEXOS eddy-correlation measurements of total latent heat flux, $H_{L,T}$. As explained above, there are two tests for best fit: the average of the R_L values should be approximately 1, and the correlation coefficient of R_L with U_{N10} should be near zero. Figure 7 represents our computations of these two statistics for a range of α values. The computations shown in Figure 5, for example, led to the values in Figure 7 at $\alpha = 0$. In Figure 7, both fitting constraints agree that α is between 4.0 and 4.5. We thus choose an intermediate value, $\alpha = 4.3 \pm 0.3$, as the best fit to the HEXOS data.

With α fixed at 4.3, we next varied β and γ systematically in (10b) and again looked at the ratio R_s of measured-to-modelled sensible heat flux, $H_{s,T}$. As with latent heat, optimum values of β and γ should produce an average of R_s values

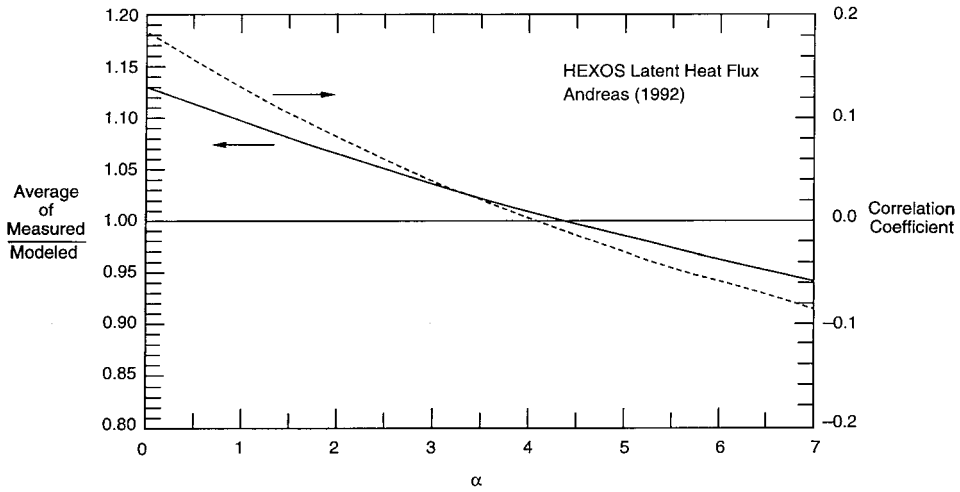

Figure 7. Evaluating α in (10a) using the HEXOS latent heat flux measurements and the Andreas (1992) spray generation function. The left vertical axis is the average of the ratio of measured-to-modelled values of latent heat flux (i.e., average of R_L values); the right vertical axis is the correlation coefficient between R_L and U_{N10}. The preferred value of α produces an average ratio near 1 and a correlation coefficient near 0.

near 1 and zero correlation between R_s and U_{N10}. We find $\beta = 6.5 \pm 0.5$ and $\gamma = 3.8 \pm 0.3$.

Figure 8 shows the results of our modelling the HEXOS heat flux data according to (10), using the Andreas (1992) spray generation function and these values of α, β, and γ. The agreement between measured and modelled fluxes is now both visually and statistically better in Figure 8 than in Figures 5 and 6. In Figure 8, both the latent and sensible heat flux ratios are more uniformly distributed about 1, and neither data cloud has the obvious slopes in Figures 5 and 6. The figure caption lists the average values of the two flux ratios and their correlations with wind speed.

The filled circles in the two panels in Figure 8 denote cases for which $|\alpha \bar{Q}_L / H_L|$ or $|[\beta \bar{Q}_S - (\alpha - \gamma)\bar{Q}_L]/H_s|$ are 10% or greater – that is, cases for which the magnitude of the modelled spray flux is at least 10% of the modelled interfacial flux. All points for wind speeds above 15 m s^{-1} in both panels are filled. Consequently, when viewed in the context of Andreas's (1992) spray model and the COARE bulk flux algorithm, the HEXOS heat flux data do contain evidence of significant sea spray effects. Probably not coincidentally, a wind speed of 15 m s^{-1} corresponds to the nominal transition to Beaufort Force 7, termed 'near gale,' when the 'sea heaps up and white foam from breaking waves begins to be blown in streaks along the direction of the wind' (e.g., Roll, 1965, p. 24).

The sensible heat flux panel in Figure 8 shows many more filled circles at low wind speeds than does the latent heat flux panel. This result highlights a consequence of spray heat transfer that few appreciate. As (6) shows, the spray sensible heat transfer is driven by $T_w - T_{ev}$. For ocean spray droplets, that evaporating

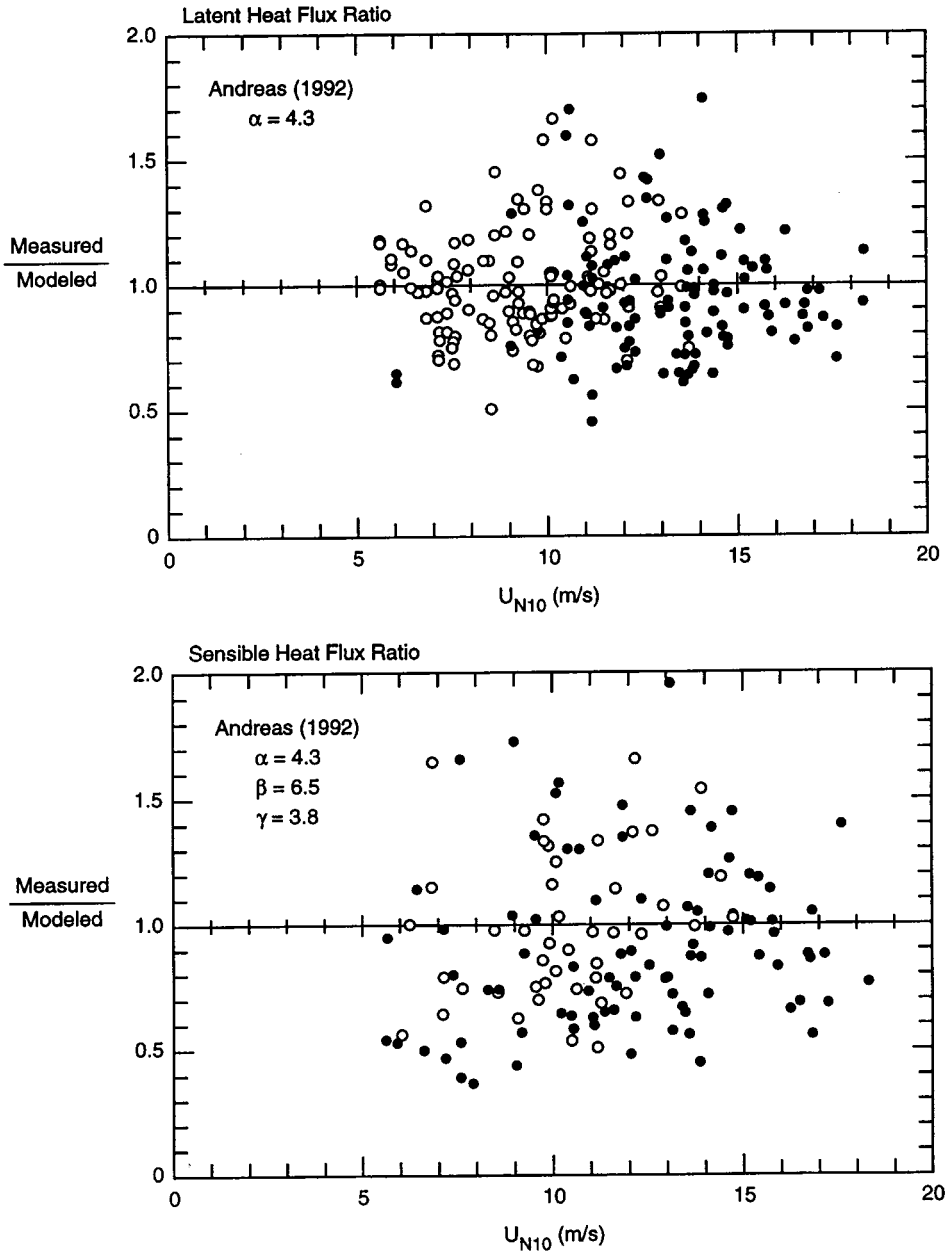

Figure 8. As in Figure 5, except here we use the Andreas (1992) function to predict spray production, and we model spray contributions to the measured heat fluxes using (10) with $\alpha = 4.3$, $\beta = 6.5$, and $\gamma = 3.8$. In the latent heat flux plot, the average of the ratios is 1.004, and the R_L-U_{N10} correlation coefficient is -0.007; in the sensible heat flux plot, the average is 0.996, and the correlation coefficient is 0.062. The filled circles denote cases for which the modelled spray contribution (the α, β, and γ terms in (10)) sum to at least 10% of the modelled interfacial fluxes (the H_s and H_L terms in (10)).

temperature T_{ev} is less than the air temperature if the relative humidity is less than about 98% (Andreas, 1995). As a result, whenever the ocean is warmer than the air and spray is present, a positive spray-mediated sensible heat flux is possible. Even when the ocean and air have the same temperature and there would, consequently, be no interfacial sensible heat flux (i.e., see (11a)), spray can still transfer sensible heat.

During HEXOS, the measured sensible heat fluxes were only moderate; the largest measured flux was 113 W m^{-2}, and only 32 of the 136 points shown in the sensible heat flux panel in Figure 8 represent fluxes larger than 50 W m^{-2}. The measured latent heat fluxes, in contrast, were large. The largest latent heat flux measured was 374 W m^{-2}, and 116 of the 233 points plotted in the latent heat flux panel in Figure 8 represent fluxes of at least 100 W m^{-2}. Because of the small sensible heat fluxes and the fact that $T_w - T_{ev}$, rather than the sea-air temperature difference, drives the spray sensible heat flux, the spray flux was more likely to be at least 10% of the interfacial heat flux in the sensible heat panel in Figure 8, even in low winds, than in the latent heat panel. In other words, the relative magnitudes of the spray and interfacial fluxes and their different scalings explains why a higher percentage of the circles at lower wind speeds are filled in the sensible heat flux panel in Figure 8 than in the latent heat flux panel.

Obtaining Figure 8 was a primary reason why we undertook this study. Katsaros and de Leeuw (1994) had contended that the Andreas (1992) spray model was incompatible with the HEXOS data, and that it predicted far larger spray fluxes than were evident in the HEXOS flux measurements. Andreas (1994b) therefore offered to test his spray model directly against the HEXOS data, which is what Figure 8 does. Our finding that α, β, and γ are all of order one implies that the Andreas (1992) model is yielding spray fluxes of the correct order and gives credence to our calling $\bar{Q}_L$ and $\bar{Q}_S$ the 'nominal' spray fluxes.

In essence, (10) represents a new way to model the air-sea heat fluxes that is especially appropriate in high winds. As in low winds, the cornerstone of this model is a bulk aerodynamic parameterization for H_s and H_L – in our case, the COARE algorithm (Fairall et al., 1996b). But we add a spray component with fitting parameters based on the HEXOS data set and the Andreas (1992) spray generation function. Andreas (1989, 1992) gives the details necessary to compute $\bar{Q}_S$, $\bar{Q}_L$, and the spray generation function required in (10).

5. Discussion

According to (10), the total turbulent heat flux (the total enthalpy flux) at the top of the DEL is

$$H_{s,T} + H_{L,T} = H_s + H_L + \beta \bar{Q}_S + \gamma \bar{Q}_L. \tag{19}$$

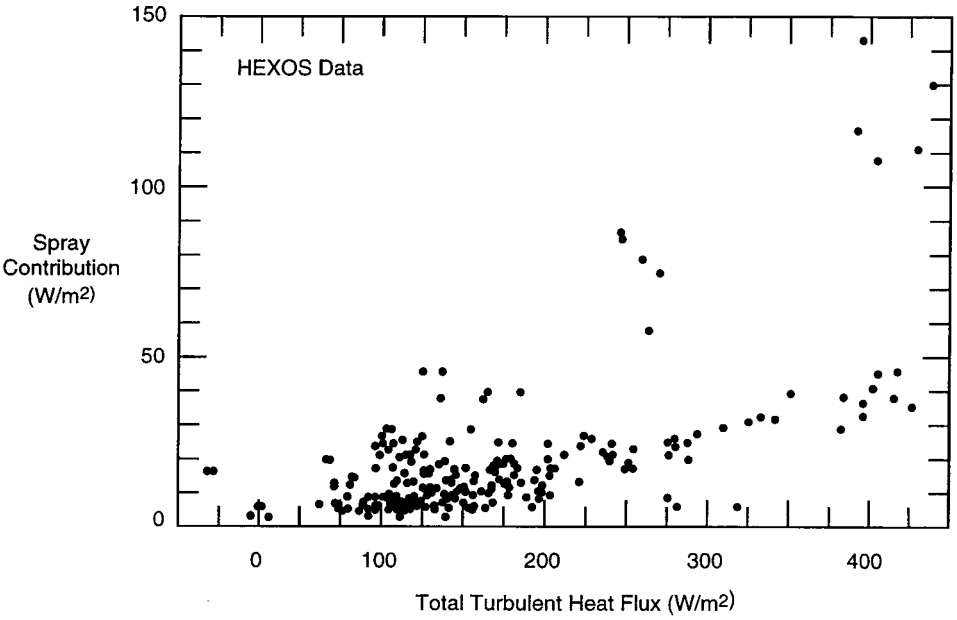

Figure 9. The spray contribution, $\beta \bar{Q}_S + \gamma \bar{Q}_L$, to the total turbulent air-sea flux is plotted against the HEXOS measurements of that total turbulent flux, $H_{s,T} + H_{L,T}$.

Note that the largest spray term in (10), $\alpha \bar{Q}_L$, has cancelled out here. As we discussed, the temperature field must supply the latent heat required to evaporate spray droplets. This is the effect that Emanuel (1995) is seeing when he states that 'spray cannot directly affect the enthalpy transfer from the ocean'.

For normal oceanic conditions, however, the two remaining spray terms in (19) are both positive. The sum $\beta \bar{Q}_S + \gamma \bar{Q}_L$ is, therefore, the amount that sea spray enhances the total air-sea enthalpy transfer.

Figure 9 demonstrates the magnitude of this spray contribution on the basis of our partitioning of the HEXOS data (as depicted in Figure 8). In Figure 9, we plot the spray contribution, $\beta \bar{Q}_S + \gamma \bar{Q}_L$, to the total turbulent heat flux versus the HEXOS measurements of that turbulent flux, $H_{s,T} + H_{L,T}$. For large turbulent fluxes (i.e., for high winds), the spray contribution increases with the total flux. Here the spray contribution is about 10% of the total turbulent flux; but in 10 cases that are obvious outliers, the spray contribution is 20–30% of the total flux. There is nothing meteorologically or instrumentally unusual about these 10 cases except they correspond to 10 of the 14 highest wind speed runs and have significant wave heights that are among the highest in our data set. Both characteristics suggest enhanced spray-mediated heat fluxes. The fact that five of these cases are not associated with runs having the largest total turbulent heat fluxes again emphasizes that the spray and interfacial fluxes scale with different variables.

Realize, too, that our spray partitioning does not depend on our spray model. From (19), we could just as well have estimated the spray contribution from

$$\beta \bar{Q}_S + \gamma \bar{Q}_L = (H_{s,T} + H_{L,T}) - (H_s + H_L). \tag{20}$$

That is, we could simply subtract the COARE algorithm estimates of H_s and H_L from the measurements. Although the run-to-run details in Figure 9 may have been different if we had estimated the spray contribution this way, the general trend would still be there.

Not surprisingly, neither the β nor the γ term in (19) is widely appreciated. For example, in concluding that the HEXOS data show no evidence of spray effects, Makin (1998) ironically ignores the sensible heat carried by the spray (the β term) in his model. The γ term in (19) is how we model the positive feedback between the temperature and moisture fields in the DEL. Evidently, Katsaros and DeCosmo (1990) and Katsaros and de Leeuw (1994) were the first to hypothesize such a feedback process. In brief, the evaporating spray cools the DEL; but bulk parameterizations based on measurements at a 10-m reference level implicitly assume low-level temperature profiles that do not exhibit this cooling (see, for example, Mestayer and Lefauconnier, 1988; Rouault et al., 1991; Edson and Fairall, 1994; Andreas et al., 1995; Edson et al., 1996; Kepert et al., 1999) and, therefore, underestimate the true interfacial sensible heat flux, H_s. The $\gamma \bar{Q}_L$ term adds this missing flux to the DEL.

Emanuel (1995) qualifies his conclusion that spray cannot affect air-sea enthalpy transfer by adding 'if $C_H = C_E$'. Bortkovskii (1987) added to the sea spray controversy by implying with his Figure 3.10 that air-sea heat exchange during storms can be modelled with single-valued C_E and C_H functions. In considering (10), however, we realize that, in high winds, $H_{s,T}$ and $H_{L,T}$ cannot be parameterized with single-valued C_H and C_E functions. Andreas (1994b) and Fairall et al. (1994) already pointed this out. In (10a), for example, the $\bar{Q}_L$ term does not scale with $q_w - q_{10}$ as the H_L term does; q_w has no effect at all on $\bar{Q}_L$ because spray droplets are at a temperature near T_{ev} as they evaporate. Consequently, $\bar{Q}_L$ depends on q_{10} or the relative humidity alone, and this dependence varies with droplet size. $\bar{Q}_L$ also depends strongly and explicitly on air temperature (see Figure 2), while H_L does not. Likewise, in (10b), $\bar{Q}_S$ scales with $T_w - T_{ev}$, where T_{ev} depends on T_{10}, the relative humidity, the seawater salinity, and droplet radius, while H_s scales with $T_w - T_{10}$. Andreas (1995) demonstrates how different T_{ev} and T_{10} can be. In (10b), the $\bar{Q}_L$ term adds to $H_{s,T}$ additional dependencies on air temperature and on q_{10} or relative humidity that are not contained in the H_s term. Finally, both $\bar{Q}_L$ and $\bar{Q}_S$ scale with ρ_s, the seawater density, while H_L and H_s scale with ρ_a, the air density.

In summary, parameterizing $H_{L,T}$ and $H_{s,T}$ in high winds in terms of C_E and C_H is unjustified because these are multivalued functions of all the environmental variables. Implementing this type of parameterization would require tables of C_E

and C_H values computed for all possible combinations of wind speed, relative humidity, and air and water temperatures.

Looking at the total turbulent flux at the top of the DEL, as in (19), seems to diminish the spray effects because the $\alpha \bar{Q}_L$ terms in (10) cancel out. A related conclusion, though, is that spray is very effective in redistributing the interfacial heat fluxes between the temperature and moisture fields in the marine boundary layer.

The hurricane community has long recognized the need for enhanced surface sensible and latent heat fluxes in high winds to generate and maintain tropical cyclones (e.g., Riehl, 1954, p. 287; Ooyama, 1982; Emanuel, 1986, 1995; Smith, 1997). Equations (10) or (19) may finally parameterize the source of this heat. In fact, in their tropical cyclone model, Fairall et al. (1994) could not obtain the proper radial temperature distribution in their cyclone boundary layer unless they incorporated spray effects with a model similar to (10) or added another mechanism for latent heat conversion, such as rain.

6. Conclusions

Original analyses of the HEXOS heat flux data did not find the dramatic increase in the bulk transfer coefficients for sensible and latent heat, C_{HN10} and C_{EN10}, for wind speeds above 15 m s^{-1} that Bortkovskii (1987) had predicted would be a consequence of sea spray. But because, theoretically, C_{HN10} and C_{EN10} should decrease with increasing wind speed at the HEXOS site in the absence of spray (see Figure 4), we suggest that the constant HEXOS values of C_{HN10} and C_{EN10} reported could reflect flux contributions from sea spray. We have, therefore, looked again at the HEXOS data for evidence of spray-mediated transfer.

Our premise is that, if there is no spray signal, state-of-the-art bulk flux algorithms should be able to reproduce the measured HEXOS sensible and latent heat fluxes. Figures 5 and 6, however, show that neither the COARE (Fairall et al., 1996b) nor the Zeng et al. (1998) algorithms, even when we account for the shallow-water HEXOS site, can predict the average magnitudes of the HEXOS sensible and latent heat fluxes or their dependence on wind speed. The Zeng et al. algorithm, in particular, over predicts both fluxes in high winds, a behaviour that makes it incompatible with our conceptual model of spray's effects. We interpret the under prediction of the COARE algorithm, on the other hand, to be the second piece of evidence suggesting that spray affects the HEXOS sensible and latent heat fluxes.

We corroborate this interpretation by complementing the COARE algorithm with a microphysical model that estimates the nominal heat fluxes $\bar{Q}_S$ and $\bar{Q}_L$ that can be theoretically attributed to spray. When $\bar{Q}_S$ and $\bar{Q}_L$ are multiplied by small numbers and added to the COARE algorithm's predictions of the interfacial sensible and latent heat fluxes, H_s and H_L, as in (10), we model the measured

HEXOS heat fluxes much better (see Figure 8). In other words, by accounting for spray effects through (10), we can make the measured HEXOS fluxes and the modelled fluxes equal, on average, and can explain the increase in measured fluxes with wind that the COARE algorithm alone cannot predict.

Equations (10) thus represent a unified model for estimating the air-sea sensible and latent heat fluxes that acknowledges both the interfacial and spray routes by which the sea and air exchange heat. Because the hurricane community, especially, desperately needs such a model, it would not be unreasonable to extrapolate (10) to near-hurricane-strength winds by assuming that both $\bar{Q}_S$ and $\bar{Q}_L$ increase as the cube of the wind speed (e.g., Fairall et al., 1994). Andreas and Emanuel (1999, 2000) have already begun investigating the role of spray in influencing the intensity of tropical cyclones with such a model.

Acknowledgements

We thank Wiebe Oost for providing the HEXOS wave height data, Chris Fairall for supplying FORTRAN code for the COARE flux algorithm, Emily B. Andreas for helping with the data processing, and two anonymous reviewers for insightful comments. The Office of Naval Research supported this work with contracts N0001498MP30029, N0001499MP30043, N0001400MP20031, and N0001401MP20042; the U.S. National Science Foundation supported it with grant ATM-00-01037.

Appendix A: Preprocessing the DeCosmo (1991) Data

As (11) shows, to estimate H_s and H_L by the bulk aerodynamic method requires U_{10}, T_{10}, q_{10}, T_w, and q_w. DeCosmo (1991), however, tabulates the neutral-stability, 10-m values of wind speed, temperature, and specific humidity, U_{N10}, T_{N10}, and q_{N10}. We therefore compute U_{10}, T_{10}, and q_{10} using the relations,

$$U_{10} = \frac{u_*}{k}[\ln(10/z_0) - \psi_m(10/L)], \tag{A1a}$$

$$T_{10} = T_w + \frac{t_*}{k}[\ln(10/z_T) - \psi_h(10/L)], \tag{A1b}$$

$$q_{10} = q_w + \frac{q_*}{k}[\ln(10/z_q) - \psi_h(10/L)], \tag{A1c}$$

where u_*, t_*, and q_* are the turbulent flux scales obtained from the HEXOS eddy-correlation measurements of surface stress, temperature flux, and moisture flux. That is,

$$u_* = (-\overline{uw})^{1/2}, \tag{A2a}$$

$$t_* = -\overline{wt}/u_*, \tag{A2b}$$

$$q_* = -\overline{wq}/q_*, \tag{A2c}$$

where u, w, t, and q are turbulent fluctuations in the longitudinal wind component, the vertical wind component, temperature, and specific humidity, and an overbar indicates a time average. Also in (A1), the Obukhov length is defined as

$$L = \left\{ \frac{-kg}{u_*^2(T_w + 273.15)} \left[t_* + \frac{0.61(T_w + 273.15)}{1 + 0.61 q_w} q_* \right] \right\}^{-1}, \tag{A3}$$

where g is the acceleration of gravity, and T_w is the temperature in °C.

DeCosmo (1991) tabulates u_*, t_*, and two values of ρ_{v*}, the moisture flux scale in terms of water vapour density: one obtained from a Lyman-alpha hygrometer and one obtained with fast-responding dry-bulb and wet-bulb thermometers. We converted ρ_{v*} to q_* for use in (A1c) and (A3) with

$$q_* = \rho_{v*}/\rho_a. \tag{A4}$$

To obtain z_0, z_T, and z_q in (A1), we used DeCosmo's (1991) tabulated values of C_{DN10}, C_{HN10}, and C_{EN10} for each HEXOS run. These yielded z_0 from (17) and z_T and z_q from (e.g., Andreas and Murphy, 1986)

$$z_T = 10 \exp\left(-\frac{k C_{DN10}^{1/2}}{C_{HN10}} \right), \tag{A5a}$$

$$z_q = 10 \exp\left(-\frac{k C_{DN10}^{1/2}}{C_{EN10}} \right), \tag{A5b}$$

which give z_T and z_q in metres.

Lastly, DeCosmo (1991) tabulates T_w. From this we calculated q_w by assuming that the vapour density at the surface was in equilibrium with seawater at T_w and salinity 34 psu. We used Buck's (1981) relations to compute the saturation vapour pressure over pure water and accounted for salinity effects in depressing the vapour pressure with the factor $1 - 0.000537S$, where S is the salinity in psu. DeCosmo tabulates a quantity identified as Q_s, but this value is again a water vapour density and has not been corrected for vapour pressure depression caused by salinity.

For the ψ_m and ψ_h functions in (A1), we used the functions DeCosmo (1991) originally used to compute U_{N10}, T_{N10}, and q_{N10} – those given in (13) and (14).

What we call the 'HEXOS data set' thus contains, after our manipulations, u_*, $H_{s,T}$ ($= -\rho_a c_p u_* t_*$), $H_{L,T}$ ($= -\rho_a L_v u_* q_*$; sometimes two values per run because of the multiple humidity sensors), T_w, q_w, U_{10}, U_{N10}, T_{10}, and q_{10}. We retain U_{N10} because this is the quantity we use to compute C_{DN10} using (16). This data set lets

us make the bulk estimates of H_s and H_L using (11) and also serves as input for our microphysical spray model.

References

Andreas, E. L.: 1989, *Thermal and Size Evolution of Sea Spray Droplets*, CRREL Report 89-11, U.S. Army Cold Regions Research and Engineering Laboratory, Hanover, NH, 37 pp. [NTIS AD-A210484.]

Andreas, E. L.: 1990, 'Time Constants for the Evolution of Sea Spray Droplets', *Tellus* **42B**, 481–497.

Andreas, E. L.: 1992, 'Sea Spray and the Turbulent Air-Sea Heat Fluxes', *J. Geophys. Res.* **97**, 11,429–11,441.

Andreas, E. L.: 1994a, 'Comments on "On the Contribution of Spray Droplets to Evaporation" by Lutz Hasse', *Boundary-Layer Meteorol.* **68**, 207–214.

Andreas, E. L.: 1994b, 'Reply', *J. Geophys. Res.* **99**, 14,345–14,350.

Andreas, E. L.: 1995, 'The Temperature of Evaporating Sea Spray Droplets', *J. Atmos. Sci.* **52**, 852–862.

Andreas, E. L.: 1996, 'Reply', *J. Atmos. Sci.* **53**, 1642–1645.

Andreas, E. L.: 1998, 'A New Sea Spray Generation Function for Wind Speeds up to 32 m s^{-1}', *J. Phys. Oceanog.* **28**, 2175–2184.

Andreas, E. L. and DeCosmo, J.: 1997, 'Partitioning the Air-Sea Heat Fluxes into Interfacial and Spray Contributions', poster presented at Fifth Scientific Meeting of The Oceanography Society, 1–4 April 1997, Seattle, WA.

Andreas, E. L. and DeCosmo, J.: 1999, 'Sea Spray Production and Influence on Air-Sea Heat and Moisture Fluxes over the Open Ocean', in G. L. Geernaert (ed.), *Air-Sea Exchange: Physics, Chemistry and Dynamics*, Kluwer Academic Publishers, Dordrecht, pp. 327–362.

Andreas, E. L. and Emanuel, K. A.: 1999, 'Effects of Sea Spray on Tropical Cyclone Intensity', in *Preprint Volume, 23rd Conference on Hurricanes and Tropical Meteorology*, 10–15 January 1999, Dallas, TX, American Meteorological Society, Boston, MA, pp. 22–25.

Andreas, E. L. and Emanuel, K. A.: 2000, 'How Sea Spray Can Affect the Intensity of Tropical Cyclones', in *Preprint Volume, 24th Conference on Hurricanes and Tropical Meteorology*, 29 May–2 June 2000, Ft. Lauderdale, FL, American Meteorololgical Society, Boston, MA, pp. J17–J18.

Andreas, E. L. and Murphy, B.: 1986, 'Bulk Transfer Coefficients for Heat and Momentum over Leads and Polynyas', *J. Phys. Oceanog.* **16**, 1875–1883.

Andreas, E. L., Edson, J. B., Monahan, E. C., Rouault, M. P., and Smith, S. D.: 1995, 'The Spray Contribution to Net Evaporation from the Sea: A Review of Recent Progress', *Boundary-Layer Meteorol.* **72**, 3–52.

Bao, J.-W., Wilczak, J. M., Choi, J.-K., and Kantha, L. H.: 2000, 'Numerical Simulations of Air-Sea Interaction under High Wind Conditions Using a Coupled Model: A Study of Hurricane Development', *Mon. Wea. Rev.* **128**, 2190–2210.

Bendat, J. S. and Piersol, A. G.: 1971, *Random Data: Analysis and Measurement Procedures*, Wiley-Interscience, New York, 407 pp.

Bohren, C. F.: 1987, *Clouds in a Glass of Beer: Simple Experiments in Atmospheric Physics*, John Wiley and Sons, New York, 195 pp.

Bortkovskii, R. S.: 1987, *Air-Sea Exchange of Heat and Moisture during Storms*, D. Reidel, Dordrecht, 194 pp.

Brutsaert, W.: 1975, 'The Roughness Length for Water Vapor, Sensible Heat, and Other Scalars', *J. Atmos. Sci.* **32**, 2028–2031.

Brutsaert, W.: 1982, *Evaporation into the Atmosphere: Theory, History, and Applications*, D. Reidel, Dordrecht, 299 pp.

Buck, A. L.: 1981, 'New Equations for Computing Vapor Pressure and Enhancement Factor', *J. Appl. Meteorol.* **20**, 1527–1532.

Chang, H.-R. and Grossman, R. L.: 1999, 'Evaluation of Bulk Surface Flux Algorithms for Light Wind Conditions Using Data from the Coupled Ocean-Atmosphere Response Experiment (COARE)', *Quart. J. Roy. Meteorol. Soc.* **125**, 1551–1588.

Davidson, K. L., Houlihan, T. M., Fairall, C. W., and Schacher, G. E.: 1978, 'Observation of the Temperature Structure Function Parameter, C_T^2, over the Ocean', *Boundary-Layer Meteorol.* **15**, 507–523.

DeCosmo, J.: 1991, *Air-Sea Exchange of Momentum, Heat and Water Vapor over Whitecap Sea States*, Ph.D. Thesis, University of Washington, Seattle, 212 pp.

DeCosmo, J., Katsaros, K. B., Smith, S. D., Anderson, R. J., Oost, W. A., Bumke, K., and Chadwick, H.: 1996, 'Air-Sea Exchange of Water Vapor and Sensible Heat: The Humidity Exchange over the Sea (HEXOS) Results', *J. Geophys. Res.* **101**, 12,001–12,016.

Donlon, C. J. and Robinson, I. S.: 1997, 'Observations of the Oceanic Thermal Skin in the Atlantic Ocean', *J. Geophys. Res.* **102**, 18,585–18,606.

Earle, M. D.: 1979, 'Practical Determinations of Design Wave Conditions', in M. D. Earle and A. Malahoff (eds.), *Ocean Wave Climate*, Plenum Press, New York, pp. 39–60.

Edson, J. B. and Andreas, E. L.: 1997, 'Modeling the Role of Sea Spray on Air-Sea Heat and Moisture Exchange', in *Preprint Volume, 12th Symposium on Boundary Layers and Turbulence*, 28 July–1 August 1997, Vancouver, B.C., American Meteorological Society, Boston, MA, pp. 490–491.

Edson, J. B. and Fairall, C. W.: 1994, 'Spray Droplet Modeling: 1. Lagrangian Model Simulation of the Turbulent Transport of Evaporating Droplets', *J. Geophys. Res.* **99**, 25,295–25,311.

Edson, J. B., Anquentin, S., Mestayer, P. G., and Sini, J. F.: 1996, 'Spray Droplet Modeling: 2. An Interactive Eulerian-Lagrangian Model of Evaporating Spray Droplets', *J. Geophys. Res.* **101**, 1279–1293.

Emanuel, K. A.: 1986, 'An Air-Sea Interaction Theory for Tropical Cyclones. Part I: Steady-State Maintenance', *J. Atmos. Sci.* **43**, 585–604.

Emanuel, K. A.: 1995, 'Sensitivity of Tropical Cyclones to Surface Exchange Coefficients and a Revised Steady-State Model Incorporating Eye Dynamics', *J. Atmos. Sci.* **52**, 3969–3976.

Fairall, C. W., Bradley, E. F., Godfrey, J. S., Wick, G. A., Edson, J. B., and Young, G. S.: 1996a, 'Cool-Skin and Warm-Layer Effects on Sea Surface Temperature', *J. Geophys. Res.* **101**, 1295–1308.

Fairall, C. W., Bradley, E. F., Rogers, D. P., Edson, J. B., and Young, G. S.: 1996b, 'Bulk Parameterization of Air-Sea Fluxes for Tropical Ocean-Global Atmosphere Coupled-Ocean Atmosphere Response Experiment', *J. Geophys. Res.* **101**, 3747–3764.

Fairall, C. W., Davidson, K. L., and Schacher, G. E.: 1979, 'Humidity Effects and Sea Salt Contamination of Atmospheric Temperature Sensors', *J. Appl. Meteorol.* **18**, 1237–1239.

Fairall, C. W., Kepert, J. D., and Holland, G. J.: 1994, 'The Effect of Sea Spray on Surface Energy Transports over the Ocean', *Global Atmos. Ocean Sys.* **2**, 121–142.

Friedlander, S. K.: 1977, *Smoke, Dust and Haze: Fundamentals of Aerosol Behavior*, John Wiley and Sons, New York, 317 pp.

Garratt, J. R.: 1992, *The Atmospheric Boundary Layer*, Cambridge University Press, Cambridge, 316 pp.

Geernaert, G. L., Katsaros, K. B., and Richter, K.: 1986, 'Variation of the Drag Coefficient and its Dependence on Sea State', *J. Geophys. Res.* **91**, 7667–7679.

Geernaert, G. L., Larsen, S. E., and Hansen, F.: 1987, 'Measurements of the Wind Stress, Heat Flux, and Turbulence Intensity during Storm Conditions over the North Sea', *J. Geophys. Res.* **92**, 13,127–13,139.

Grant, A. L. M. and Hignett, P.: 1998, 'Aircraft Observations of the Surface Energy Balance in TOGA-COARE', *Quart. J. Roy. Meteorol. Soc.* **124**, 101–122.

Hasse, L.: 1992, 'On the Contribution of Spray Droplets to Evaporation', *Boundary-Layer Meteorol.* **61**, 309–313.

Katsaros, K. B. and DeCosmo, J.: 1990, 'Evaporation in High Wind Speeds, Sea Surface Temperature at Low Wind Speeds, Examples of Atmospheric Regulation', in P. G. Mestayer, E. C. Monahan, and P. A. Beetham (eds.), *Modelling the Fate and Influence of Marine Spray*, Marine Sciences Institute, University of Connecticut, Groton, pp. 106–114.

Katsaros, K. B. and de Leeuw, G.: 1994, 'Comment on "Sea Spray and the Turbulent Air-Sea Heat Fluxes" by Edgar L Andreas', *J. Geophys. Res.* **99**, 14,339–14,343.

Katsaros, K. B., DeCosmo, J., Lind, R. J., Anderson, R. J., Smith, S. D., Kraan, R., Oost, W., Uhlig, K., Mestayer, P. G., Larsen, S. E., Smith, M. H., and de Leeuw, G.: 1994, 'Measurements of Humidity and Temperature in the Marine Environment during the HEXOS Main Experiment', *J. Atmos. Oceanic Tech.* **11**, 964–981.

Katsaros, K. B., Smith, S. D., and Oost, W. A.: 1987, 'HEXOS-Humidity Exchange over the Sea, a Program for Research on Water-Vapor and Droplet Fluxes from Sea to Air at Moderate to High Wind Speeds', *Bull. Amer. Meteorol. Soc.* **68**, 466–476.

Kepert, J. D.: 1996, 'Comments on "The Temperature of Evaporating Sea Spray Droplets" ', *J. Atmos. Sci.* **53**, 1634–1641.

Kepert, J. D., Fairall, C. W., and Bao, J.-W.: 1999, 'Modelling the Interaction between the Atmospheric Boundary Layer and Evaporating Sea Spray Droplets', in G. L. Geernaert (ed.), *Air-Sea Exchange: Physics, Chemistry and Dynamics*, Kluwer Academic Publishers, Dordrecht, pp. 363–409.

Kinsman, B.: 1965, *Wind Waves*, Prentice-Hall, Englewood Cliffs, NJ, 676 pp.

Large, W. G. and Pond, S.: 1981, 'Open Ocean Momentum Flux Measurements in Moderate to Strong Winds', *J. Phys. Oceanog.* **11**, 324–336.

Ling, S. C.: 1993, 'Effect of Breaking Waves on the Transport of Heat and Water Vapor Fluxes from the Ocean', *J. Phys. Oceanog.* **23**, 2360–2372.

Liu, W. T., Katsaros, K. B., and Businger, J. A.: 1979, 'Bulk Parameterization of Air-Sea Exchanges of Heat and Water Vapor Including the Molecular Constraints at the Interface', *J. Atmos. Sci.* **36**, 1722–1735.

Maat, N., Kraan, C., and Oost, W. A.: 1991, 'The Roughness of Wind Waves', *Boundary-Layer Meteorol.* **54**, 89–103.

Makin, V. K.: 1998, 'Air-Sea Exchange of Heat in the Presence of Wind Waves and Spray', *J. Geophys. Res.* **103**, 1137–1152.

Mestayer, P. and Lefauconnier, C.: 1988, 'Spray Droplet Generation, Transport, and Evaporation in a Wind Wave Tunnel during the Humidity Exchange over the Sea Experiments in the Simulation Tunnel', *J. Geophys. Res.* **93**, 572–586.

Mestayer, P. G., Edson, J. B., Fairall, C. W., Larsen, S. E., and Spiel, D. E.: 1989, 'Turbulent Transport and Evaporation of Droplets Generated at an Air-Water Interface', in J.-C. André, J. Cousteix, F. Durst, B. E. Launder, F. W. Schmidt, and J. H. Whitelaw (eds.), *Turbulent Shear Flows 6*, Springer-Verlag, Berlin, pp. 129–147.

Mestayer, P. G., Van Eijk, A. M. J., de Leeuw, G., and Tranchant, B.: 1996, 'Numerical Simulation of the Dynamics of Sea Spray over the Waves', *J. Geophys. Res.* **101**, 20,771–20,797.

Miller, M. A.: 1987, *An Investigation of Aerosol Generation in the Marine Planetary Boundary Layer*, M.S. Thesis, The Pennsylvania State University, University Park, 142 pp.

Ooyama, K. V.: 1982, 'Conceptual Evolution of the Theory and Modeling of the Tropical Cyclone', *J. Meteorol. Soc. Japan* **60**, 369–379.

Pruppacher, H. R. and Klett, J. D.: 1978, *Microphysics of Clouds and Precipitation*, D. Reidel, Dordrecht, 714 pp.

Riehl, H.: 1954, *Tropical Meteorology*, McGraw-Hill, New York, 392 pp.

Roll, H. U.: 1965, *Physics of the Marine Atmosphere*, Academic Press, New York, 426 pp.

Rouault, M. P., Mestayer, P. G., and Schiestel, R.: 1991, 'A Model of Evaporating Spray Droplet Dispersion', *J. Geophys. Res.* **96**, 7181–7200.

Schmitt, K. F., Friehe, C. A., and Gibson, C. H.: 1978, 'Humidity Sensitivity of Atmospheric Temperature Sensors by Salt Contamination', *J. Phys. Oceanog.* **8**, 151–161.

Smith, M. H., Park, P. M., and Consterdine, I. E.: 1993, 'Marine Aerosol Concentrations and Estimated Fluxes over the Sea', *Quart. J. Roy. Meteorol. Soc.* **119**, 809–824.

Smith, R. K.: 1997, 'On the Theory of CISK', *Quart. J. Roy. Meteorol. Soc.* **123**, 407–418.

Smith, S. D.: 1990, 'Influence of Droplet Evaporation on HEXOS Humidity and Temperature Profiles', in P. G. Mestayer, E. C. Monahan, and P. A. Beetham (eds.), *Modelling the Fate and Influence of Marine Spray*, Marine Sciences Institute, University of Connecticut, Groton, pp. 171–174.

Smith, S. D., Anderson, R. J., Oost, W. A., Kraan, C., Maat, N., DeCosmo, J., Katsaros, K. B., Davidson, K. L., Bumke, K., Hasse, L., and Chadwick, H.: 1992, 'Sea Surface Wind Stress and Drag Coefficients: The HEXOS Results', *Boundary-Layer Meteorol.* **60**, 109–142.

Smith, S. D., Katsaros, K. B., Oost, W. A., and Mestayer, P. G.: 1990, 'Two Major Experiments in the Humidity Exchange over the Sea (HEXOS) Program', *Bull. Amer. Meteorol. Soc.* **71**, 161–172.

Smith, S. D., Katsaros, K. B., Oost, W. A., and Mestayer, P. G.: 1996, 'The Impact of the HEXOS Programme', *Boundary-Layer Meteorol.* **78**, 121–141.

Van Eijk, A. M. J., Tranchant, B. S., and Mestayer, P. G.: 2001, 'SeaCluse: Numerical Simulation of Evaporating Sea Spray Droplets', *J. Geophys. Res.* **106**, 2573–2588.

Wilson, B. W.: 1965, 'Numerical Prediction of Ocean Waves in the North Atlantic for December, 1959', *Dtsch. Hydrogr. Z.* **18**, 114–130.

Zeng, X., Zhao, M., and Dickinson, R. E.: 1998, 'Intercomparison of Bulk Aerodynamic Algorithms for the Computation of Sea Surface Fluxes using TOGA COARE and TAO Data', *J. Climate* **11**, 2628–2644.